

Infrared Spectroscopic Study of the Acidobasic Properties of Beta Zeolite

A. Vimont, F. Thibault-Starzyk,* and J. C. Lavalley

Laboratoire Catalyse et Spectrochimie, CNRS–Institut des Sciences de la Matière et du Rayonnement,
6 Boulevard du Maréchal Juin, 14050 Caen Cedex, France

Received: July 23, 1999; In Final Form: October 26, 1999

An intense and narrow infrared band was observed around 885 cm^{-1} in the spectrum of activated dealuminated beta zeolites. This band does not correspond to the vibration of a hydroxy group, as was shown by in situ deuterium exchange and heavy-water steaming of the sample in the infrared cell. It is rather linked to the vibration of a site corresponding to specific defects in the structure. Pyridine adsorption evidenced the strong Lewis character of this site. At the same time, a direct link with a $\nu(\text{OH})$ band at 3782 cm^{-1} was found. CO_2 adsorption partially transformed these OH groups into hydrogen–carbonate species, thus showing their basic properties. Assignment is proposed to a tricoordinated aluminum atom partially connected to the framework, with a hydroxy group on the aluminum atom. The electronic vacancy on the Al atom, together with the basic hydroxy group, constitutes an acid–base pair on an acidic zeolite. The 885 cm^{-1} band is a direct infrared fingerprint of a Lewis site.

1. Introduction

Zeolite beta is an active catalyst for many industrial reactions such as hydrocarbons alkylation and catalytic cracking.^{1,2} Organic synthesis is, however, the domain where its catalytic properties are the most interesting such as in aromatics acylation and Meerwein–Ponndorf–Verley reaction.^{3–7} Localization, nature, and catalytic role of the active sites for most of these reactions remain up to now an open question.^{3,7,8} This has motivated many spectroscopic studies (IR and NMR) of beta zeolites, and it has been shown that the aluminum state in the framework as well as Brønsted and Lewis acidity are very complex for these materials.

There are only a few localized surface sites which spectroscopic techniques can directly detect. Apart from Brønsted sites, for which the infrared pattern is well-known, other types of sites reported are siloxane bridges on silica heated above 875 K (infrared bands at 888 , 908 , and 940 cm^{-1})^{9,10} and surface defects on alumina (infrared band at 1050 cm^{-1}).^{11,12} These two sites are respectively affected by adsorption of water, pyridine, or alcohols, and water, hydrogen sulfide, ammonia, or alcohols. A site similar to that on silica was reported on pure silicalite, leading to an infrared band at 890 cm^{-1} . It was affected by methanol but not by CO adsorption.^{13,14}

This spectral region ($600\text{--}1200\text{ cm}^{-1}$) is difficult to observe for activated catalysts. This part of the spectrum presents intense infrared absorptions, because of Si–O and Al–O structure vibrations in zeolites, other silicates, and aluminosilicates. The samples are therefore studied as mixtures with KBr, and hydrated solids are generally studied. A band around 960 cm^{-1} has been observed in the infrared or Raman spectrum of Ti–silicalites outgassed at room temperature.¹⁵ Several assignments were proposed: $\nu(\text{Ti}=\text{O})$, $\nu(\text{Si}-\text{O}-\text{Ti})$, or hydroxy groups $\nu(\text{Si}-\text{OH})$ vibrations.^{16–18} This band is affected (shifted toward higher wavenumbers and broadened) by adsorption of water, ammonia or methanol.¹⁸ It is shifted by H_2^{17}O and H_2^{18}O exchange to 952 and 937 cm^{-1} , but is not affected by

deuteration,¹⁹ and has therefore been finally assigned to a $\nu_{\text{as}}(\text{Si}-\text{O}-\text{Ti})$ vibration, associated to four-coordinated Ti. On Al–beta zeolite, theoretical computations confirm the distorted geometry of framework aluminum atoms,²⁰ as deduced from NMR results. ^{27}Al NMR experiments had shown that the environment of aluminum atoms, in the beta zeolite framework, could be changed from tetrahedral to octahedral upon calcination of an ammonium zeolite, and this change was reversible in the presence of ammonia, pyridine, or after ionic exchange.²¹ Addition of water to such distorted sites could lead to octahedral aluminum atoms²² or to their hydrolysis, and yield the so-called “invisible” aluminum atoms. The deformation of unstable aluminum sites upon temperature variation has also been suggested by ^1H NMR.²³ Original hydroxy groups detected by infrared spectroscopy at too high a wavenumber (3780 cm^{-1}) for zeolitic hydroxyls were tentatively assigned to OH bound to three-coordinated aluminum atoms,²⁴ but no infrared pattern has been reported up to now for this particular aluminum.

We describe here a new band in the infrared spectrum of zeolite beta around 885 cm^{-1} . We present its assignment and the behavior of the corresponding site in the zeolite, upon thermal and hydrothermal treatment of various samples, and upon adsorption of carbon dioxide and pyridine.

2. Experimental Section

Our samples had two distinct origins. The first was a commercial beta zeolite (PQ, Si/Al = 12.5); it was calcined in dry air at 773 , 973 , and 1173 K to yield samples BEA500, BEA700, and BEA900, respectively. Crystallinity measured by X-ray diffraction (XRD) was slightly affected for BEA700, and greatly for BEA900. The second sample type (denoted as SD1) was provided by the Institut Français du Pétrole. It was synthesized in fluorine medium²⁵ and calcined at 823 K under air (diluted in a N_2 flow) for 6 h so as to control the template decomposition and avoid damaging the structure. The protonic form was thus obtained without ammonium exchange. Physical and chemical data are presented in Table 1.

* To whom correspondence should be addressed (E-mail: fts@ismra.fr).

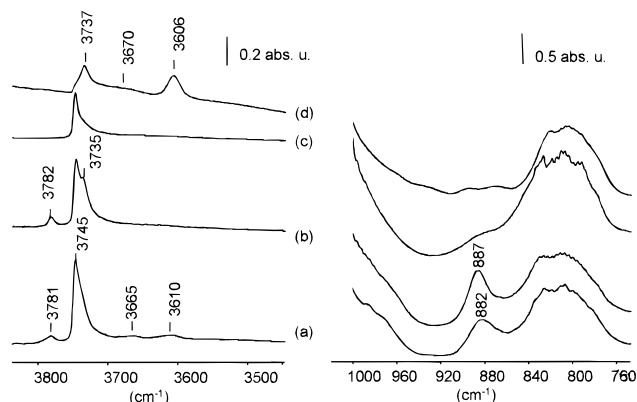


Figure 1. Infrared spectra of activated beta zeolites: (a) BEA500; (b) BEA700; (c) BEA900; and (d) SD1.

TABLE 1: Beta Zeolites Samples

	BEA 500	BEA 700	BEA 900	BEA SD1
Si/Al global	12.5	12.5	12.5	19
S_{BET} (m ² /g)	697	637	422	420
NMR ²⁷ Al				
Al ^{IV} (%)	73	69	56	—
Al ^V (%)	0	0	14	—
Al ^{VI} (%)	27	31	30	—

Infrared transmission spectra were recorded on self-supporting wafers (2 cm², 6–10 mg, prepared by application of a pressure of $5 \cdot 10^7$ Pa during 10 min). The wafers were placed into an infrared quartz cell allowing heating of the sample as well as introduction of known quantities of gas. The catalysts were activated under vacuum (10^{-6} Torr) by slow heating ($1 \text{ K} \cdot \text{min}^{-1}$) up to 723 K. Spectra were recorded at room temperature using a Nicolet Magna 750 with 4 cm^{-1} optical resolution and one level zero-filling.

Deuterium exchange of zeolite samples was done in mild conditions by heating the catalyst in the infrared cell in the presence of D₂O (15 Torr) at 393 K, followed by progressive heating and evacuation down to 10^{-6} Torr at 673 K.

Steaming was done (after deuterium exchange when necessary) by heating the catalyst with H₂O or D₂O (15 Torr) at 873 K in the infrared cell during 14 h.

Residual water traces were removed from the cell by argon flushing before adsorption of probe molecules. Pyridine adsorption was done by introducing in the cell known doses of the probe molecule at 440 K. CO₂ adsorption (10 Torr) was done at room temperature. CO₂ was dried in a liquid nitrogen cold trap, and pyridine was dried on molecular sieves.

3. Results

3.1. Activated Catalysts. Infrared spectra of activated catalysts are displayed in Figure 1. An intense and narrow band around 885 cm^{-1} is in some cases clearly visible near the structure bands at 1000 and 820 cm^{-1} . The intensity of the 885 cm^{-1} band is zero on SD1, more important on BEA700 than on BEA500, and is very small on BEA900. Samples are generally studied in this spectral region as KBr pellets, and Figure 2 shows that in this case the 885 cm^{-1} band remains invisible: this is a general phenomenon in hydrated samples and the band is only detected after activation. Influence of water on the 885 cm^{-1} band will be presented in a forthcoming paper.

Features for hydroxy groups appear above 3500 cm^{-1} . Bridged OH groups are visible in the spectra of BEA500 and SD1 at $3605\text{--}3610 \text{ cm}^{-1}$. A weak and large band around 3665 cm^{-1} also exists on these catalysts (discussed in a previous

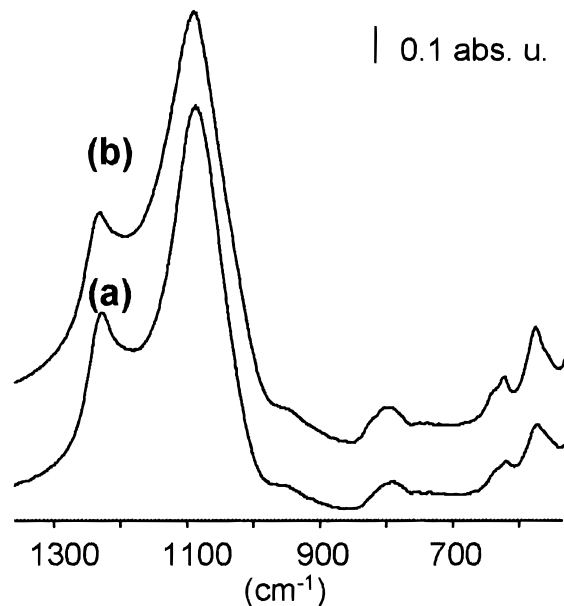


Figure 2. Infrared spectra of diluted samples (2% in KBr) in the structure band region: (a) BEA500; (b) BEA700.

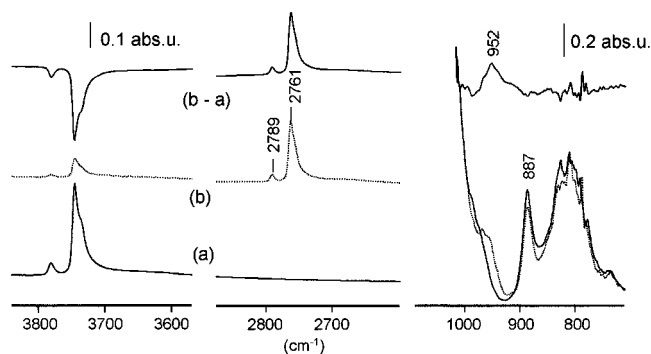


Figure 3. Infrared spectra of BEA700 zeolite after (a) activation; (b) deuterium exchange by D₂O at 393 K (dotted line).

paper²⁶). Bands for silanol groups are observed on all catalysts at 3735 cm^{-1} (assigned to framework default silanols²⁷) and 3745 cm^{-1} (external surface silanols). On SD1, the intensity of silanol bands is weak. On BEA900, framework default silanols seem nearly totally absent and only external surface silanols are observed. XRD, together with the reduced Brunauer–Emmett–Teller (BET) specific surface, shows that the structure was greatly amorphized after calcination at high temperature.

3.2. Deuteration. Some samples were exchanged to their deuterated form to check the assignment of the 885 cm^{-1} band to an OH vibration. Corresponding spectra are shown in Figure 3. Isotopic exchange is evidenced by an almost complete replacement of $\nu(\text{OH})$ bands in the $3500\text{--}3800 \text{ cm}^{-1}$ region by $\nu(\text{OD})$ between 2600 and 2800 cm^{-1} . Between 800 and 1000 cm^{-1} , a new band is observed at 952 cm^{-1} , assigned to $\delta(\text{SiO}-\text{D})$.²⁸ The 885 cm^{-1} band seems unaffected. However, deuterium exchange of the SD1 sample (Figure 4) leads to a new intense band at 897 cm^{-1} that could mask the disappearing of the 885 cm^{-1} band. It can be assigned to a $\delta(\text{bridged OD})$ vibration, in agreement with observations on Y zeolites.²⁹ The intensity of this band on SD1 is due to the relatively important amount of bridged hydroxy groups on this solid. To assign unambiguously the 885 cm^{-1} band, SD1 was steamed by D₂O after deuteration. The band at ca. 885 cm^{-1} appeared (882 cm^{-1} , Figure 4c) while the intensities of the $\delta(\text{OD})$ and $\nu(\text{OD})$ bands from the bridged hydroxy groups at 897 and 2660 cm^{-1} , respectively, diminished.

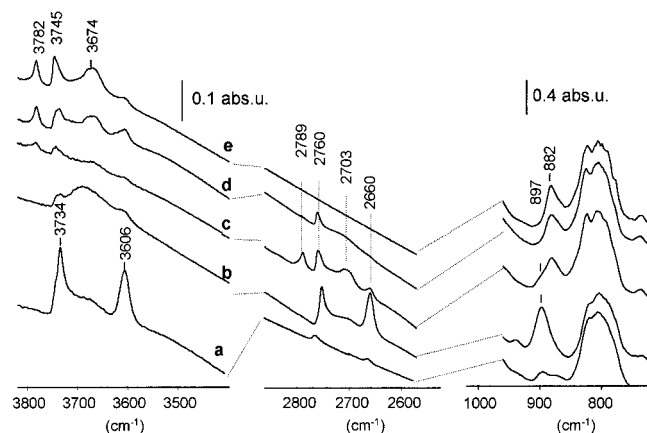


Figure 4. Infrared spectra of SD1 sample after successive (a) activation; (b) deuterium exchange; (c) 14 h steaming by D₂O at 873 K; and (d) back exchange with H₂O. Spectrum (e) is that of the normally steamed SD1 sample without isotopic effect.

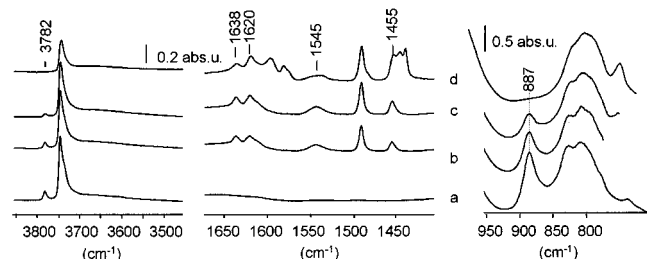


Figure 5. Infrared spectra of BEA700 sample after (a) activation; (b) 258 $\mu\text{mol}\cdot\text{g}^{-1}$ pyridine adsorption at 440 K; (c) 360 $\mu\text{mol}\cdot\text{g}^{-1}$ pyridine adsorption at 440 K; and (d) equilibration of the sample with 1 Torr pyridine.

Two new hydroxy groups appeared, with $\nu(\text{OD})$ at 2703 and 2789 cm^{-1} . Back-exchange with H₂O (Figure 4d) led to replacement of most OD groups by OH groups, with $\nu(\text{OH})$ at 3606, 3674, 3734, and 3782 cm^{-1} . The newly formed band at 882 cm^{-1} remained unaffected; it therefore does not originate in the vibration of an OH or OD group. This band appears upon steaming, as we determined by steaming with normal water (Figure 4e). It was again accompanied by new $\nu(\text{OH})$ bands at 3745, 3782 (on BEA500 and BEA700), and 3665 cm^{-1} (on BEA500), and by an intensity decrease of the framework-bridged $\nu(\text{OH})$ at 3606 cm^{-1} .

3.3. Adsorption of Probe Molecules. Zeolite samples presenting the 885 cm^{-1} band were studied by adsorption of probe molecules, chosen for showing no band in that particular region.

Infrared spectra recorded during pyridine adsorption on BEA700 are presented in Figure 5. The 885 cm^{-1} band was perturbed; it totally disappeared in the end. No new band was observed in that region. Bands for pyridinium species (1545 and 1638 cm^{-1}) and for Lewis coordinated pyridine (1455 and 1620 cm^{-1}) were visible. The 3782 cm^{-1} band gradually disappeared, whereas the silanol $\nu(\text{OH})$ bands at 3746 and 3735 cm^{-1} were also deeply perturbed. Ninety percent of the pyridinium species were desorbed under vacuum at 723 K (Figure 7), as well as 40% of the Lewis coordinated species, whereas the 885 cm^{-1} band was only slightly recovered. A new weak band (850 cm^{-1} , Figure 6) was observed on BEA700 and BEA500 (not BEA900) upon vacuum heating above 573 K (only after pyridine adsorption). After 24 h at 723 K, pyridinium species were desorbed, but some Lewis coordinated pyridine still existed on the surface (Figure 6d). The 885 cm^{-1} band remained perturbed, as well as the band at 3782 cm^{-1} and a

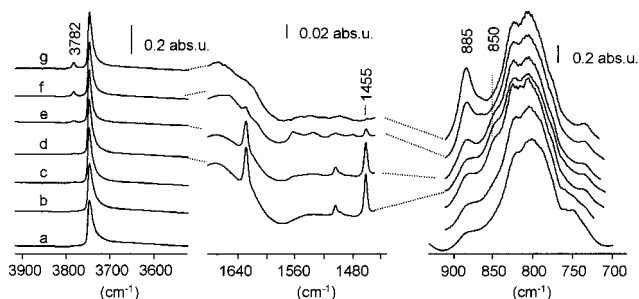


Figure 6. Infrared spectra recorded during desorption of pyridine on sample BEA700 by evacuation at the indicated temperature: (a) 473 K; (b) 573 K; (c) 723 K; (d) 24 h at 723 K; (e) 873 K; and after heating at 723 K in the presence of 160 Torr O₂ during (f) 2 h; (g) 20 h.

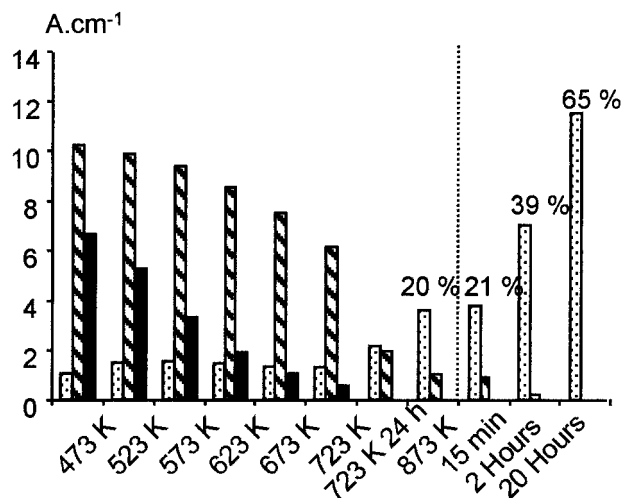


Figure 7. Quantitative analysis of spectra displayed in Figure 6. Changes in the areas of the characteristic infrared bands for protonated pyridine (1545 cm^{-1} , black), Lewis coordinated pyridine (1455 cm^{-1} , dashed, area $\times 3$), and of the 885 cm^{-1} band (dotted, area $\times 3$). The last three datasets were obtained after O₂ treatment at 723 K for the indicated period of time, followed by evacuation at the same temperature.

component of the silanols $\nu(\text{OH})$ at 3748 cm^{-1} , in agreement with previous studies.³⁰ All of these bands only reappeared after oxygen treatment at high temperature, and the intensity of the band at 850 cm^{-1} was strongly diminished. After this step, new bands could also be seen at 1474, 1492, 1529, 1550, and 1556 cm^{-1} , probably because of pyridine oxidation. Traces of impurities are visible in the infrared spectrum even after 24 h under oxygen atmosphere at high temperature. Integrated intensities of the bands at 885 and 3782 cm^{-1} are linearly linked during adsorption and elimination of pyridine (Figure 8), which suggests a correlation between the corresponding hydroxy group and the site corresponding to the 880 cm^{-1} vibration. These hydroxyls are not acidic, and they are not linked to the Brønsted sites detected by pyridine protonation. Perturbation of the 885 and 3782 cm^{-1} bands rather seems related to pyridine coordinated to strong Lewis sites.

CO₂ is a molecule used in infrared spectroscopy to probe the basicity of metal oxides. On alumina, CO₂ adsorption leads to the formation of several species: organic carbonates (bands in the 1700–1800 cm^{-1} and 1150–1250 cm^{-1} regions) and mono- and bidentate carbonates (1710–1315 cm^{-1}), because of the presence of basic sites on the surface.³¹ Interaction of CO₂ mainly occurs with surface hydroxy groups yielding hydrogen-carbonate species (four bands at 3615, 1235, 1620–1650, and 1457–1490 cm^{-1}). CO₂ adsorption on BEA500 (Figure 9) yielded, in addition to the physisorbed CO₂ $\nu(\text{OCO})$

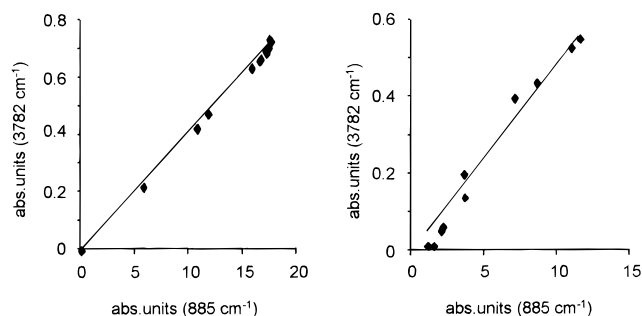


Figure 8. Integrated area for the 3782 cm^{-1} band as a function of that of the 885 cm^{-1} band during pyridine adsorption at 443 K on BEA700 (left), and during pyridine desorption as described in caption for Figure 6 (right).

bands at 1375 and $2300\text{--}2350\text{ cm}^{-1}$, two bands at 1625 and 1503 cm^{-1} which persisted after evacuation. By comparison with data obtained on alumina, they can be assigned to hydrogen-carbonates³² or monodentate carbonates.³¹ Hydrogen-carbonates are also characterized by $\delta(\text{OH})$ and $\nu(\text{OH})$ vibrations at 1235 and $3610\text{--}3620\text{ cm}^{-1}$ on alumina, but these regions are difficult to observe on zeolites. Deuterated hydrogen-carbonates (obtained on deuterated alumina) lead to typical shifts for the $\nu(\text{CO})$ bands.³³ Spectra obtained after CO_2 adsorption on deuterated BEA500 (Figure 9, spectra 2b) show two shifted bands at 1605 and 1498 cm^{-1} in agreement with a hydrogen-carbonate nature. These bands are sensitive to deuterium exchange, and therefore cannot be assigned to carbonate species. The species obtained upon CO_2 adsorption are thus hydrogen-carbonates, although $\delta(\text{OD})$ or $\delta(\text{OH})$ bands are not observed because of intense bands in the zeolites spectrum. The 885 cm^{-1} band was not affected by CO_2 adsorption. Components of the 3782 and 3746 cm^{-1} bands were, on the contrary, perturbed when hydrogen-carbonates were formed. To check a possible basicity of these hydroxy groups, which would be responsible for the hydrogen-carbonate formation, CO_2 was adsorbed in the same conditions on BEA900, which does not present the 3782 cm^{-1} band. Two weak bands were observed at 1610 and 1500 cm^{-1} , together with a small peak at 3608 cm^{-1} (Figure 9, spectra 3b). Hydrogen-carbonates are thus also detected on sample BEA900, but in very weak amounts (detection of these bands is easier on this sample which has no band for acidic hydroxyl in this region). Appearance of these hydrogen-carbonate bands on BEA900 is associated with the perturbation of a component of the silanol band at 3745 cm^{-1} .

4. Discussion

Hydroxy groups lead to a complex infrared pattern on zeolite beta. Six types of hydroxy groups are known.

- Three types of silanol groups, according to their $\nu(\text{OH})$ vibration frequency:^{26,27} $3747\text{--}3749\text{ cm}^{-1}$ (extraframework silica-alumina type SiOH), $3744\text{--}3746\text{ cm}^{-1}$ (amorphous silica or external surface SiOH), $3730\text{--}3738\text{ cm}^{-1}$ (so-called internal or structure silanols, due to defects in the structure).

- Acidic bridging OH around 3610 cm^{-1} .

- Two types of aluminic OH at $3660\text{--}3665$ and $3780\text{--}3785\text{ cm}^{-1}$, sensitive to calcination temperature³⁰ and to acid treatment.^{26,30,34} These infrared bands are assigned to extraframework silica-alumina AlOH groups,^{26,35} or to OH on partially hydrolyzed aluminum sites, bound to the framework via one or two oxygen bonds.^{24,36}

The second main group of infrared bands for zeolites is the group of structure bands, in the $600\text{--}1200\text{ cm}^{-1}$ region. Our results show that a band around 885 cm^{-1} is present on calcined

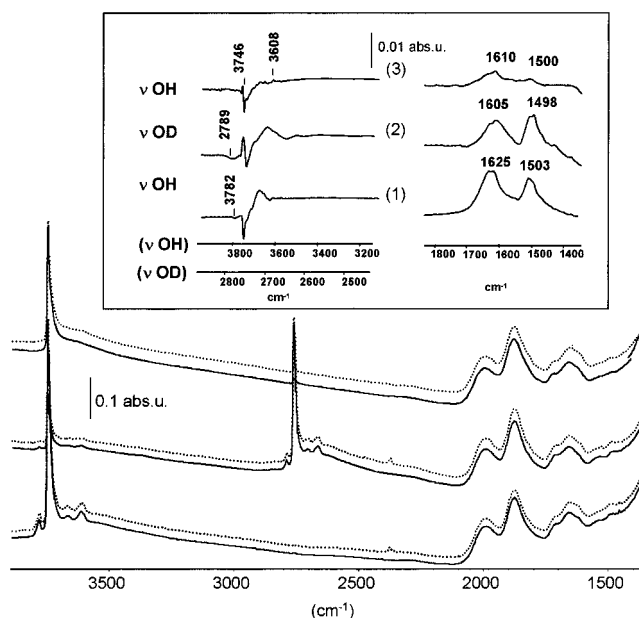


Figure 9. Infrared spectra recorded after activation at 723 K (continuous line), after equilibrating with 10 Torr CO_2 and evacuation under primary vacuum (dotted line) for samples BEA500 (1), deuterated BEA500 (2), and BEA900 (3). Insets: difference spectra showing modifications upon CO_2 adsorption.

and activated BEA500 and BEA700 samples. This band is not systematically detected on all beta zeolite samples. It is, for example, not present on SD1 sample. On this zeolite, pyridine adsorption at 473 K after activation shows a particularly weak proportion of Lewis sites: the ratio for infrared bands characterizing Lewis and Brønsted sites (1455 and 1545 cm^{-1} , respectively) is only 0.26 , and this is even clearer if no acid treatment is performed. Silanols at 3745 cm^{-1} due to framework defects are not intense and the 3782 cm^{-1} band, which is only observed after partial dealumination of the structure,²⁶ is not detected. XRD shows a good crystallinity for this sample. Noted that the acidic form of this zeolite was obtained by direct and careful calcination of the template, without intermediate ammonium exchange. It has been shown by NMR spectroscopy^{21,30,37} that calcination of the ammonium form of beta zeolite leads to damages in the structure. Infrared data, in agreement with a preserved structure, can thus be explained by a mild postsynthesis treatment. After the sample is steamed at 873 K , defects in the structure are observed: new hydroxy bands appear at 3670 and 3782 cm^{-1} , at the expense of bridging hydroxy groups at 3606 cm^{-1} , and pyridine adsorption and evacuation at 473 K shows an increased Lewis sites proportion ($A_{\text{pyL}}(1455\text{ cm}^{-1})/A_{\text{pyH}^+}(1545\text{ cm}^{-1}) = 1.13$). One can therefore propose that the 885 cm^{-1} band appeared upon steaming and is linked to structure defects not present on well-crystallized samples. The origin of this band on the steamed SD1 sample is probably the same as that of the band observed on BEA500 and BEA700. On these two samples, dealumination by calcination under air also creates defects, once more evidenced by the presence of $\nu(\text{OH})$ bands at 3665 (BEA500) and 3782 cm^{-1} (BEA500 and BEA700), as well as by the increased Lewis sites proportion, with values for $A_{\text{pyL}}(1455\text{ cm}^{-1})/A_{\text{pyH}^+}(1545\text{ cm}^{-1})$ equal to 1.53 and 2.28 for BEA500 and BEA700, respectively. It is thus confirmed that the 885 cm^{-1} band does not originate in impurities, but rather that it is linked to defects in beta zeolite, created by calcining in the presence of water traces at moderate temperature (the band is not present in the sample calcined at 1173 K) or by steaming treatments.

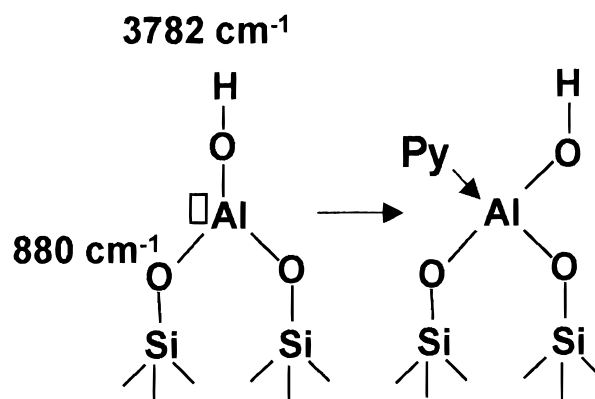
The band is situated in the transmission window between structure tetrahedrons ν_{as} and ν_{s} vibration bands. Zeolites silanol $\nu(\text{Si}-\text{O})$ and $\delta(\text{OH})$ bands are also expected in this region. The 880 cm^{-1} band could be due to one of these vibrations for a newly created silanol group that appeared during dealumination. These vibration modes would, however, be sensitive to deuteration, and be significantly shifted to lower wavenumbers upon replacement of hydrogen by deuterium.²⁸ The experiment performed with sample SD1 (deuteration followed by in situ steaming with D_2O , and back exchange with H_2O) shows that the studied band is not affected by any hydrogen isotope effect. We therefore state that the band does not originate in the vibration of an OH group, but rather in a Si–O or Al–O vibration linked to structural defects.

Pyridine Adsorption. The 885 cm^{-1} band was much affected by pyridine adsorption. At 1 Torr equilibrium pressure of pyridine, the band was not visible anymore, and it was therefore linked to an acidic site. Although protonated pyridine disappeared from the surface after desorption of pyridine by 24 h vacuum at 773 K, pyridine remained Lewis coordinated and the 880 cm^{-1} band remained 90% perturbed. This band is thus linked to strong enough Lewis sites to retain pyridine at high temperature (the 850 cm^{-1} band might be due to reversible perturbation of these sites by pyridine at high temperature; it disappears upon removal of pyridine by oxygen treatment). Using an extinction coefficient $\epsilon = 1.5\text{ }\mu\text{mol}^{-1}\cdot\text{cm}$ for the 1455 cm^{-1} band,³⁸ we obtained a maximum estimation of 6% of total aluminum content in sample BEA700. These sites are probably responsible for part of the Lewis acidity present on BEA500 and 700 samples, and created upon steaming of SD1.

A correlation was found between the intensities of the bands at 885 and 3782 cm^{-1} upon pyridine adsorption and desorption on BEA700. Assuming that the 885 cm^{-1} band is due to the vibration of only one site, we can state that the site of interest is linked to the hydroxy groups characterized by the 3782 cm^{-1} vibration. An indirect effect of Lewis sites coordination by pyridine had also been reported on the intensity of a $\nu(\text{OH})$ at 3785 cm^{-1} on alumina and on silanol groups in some zeolites.²⁷ For beta zeolite, a very weak Brønsted acidity has been shown for this hydroxy group.^{24,39} Such a weak acidity cannot justify the coordination of pyridine up to 773 K. Our experiments suggest that coordination of pyridine on the site corresponding to the 885 cm^{-1} band indirectly perturbs the 3782 cm^{-1} hydroxyl. The high frequency of this OH and its link to framework dealumination could suggest assignment of the 885 cm^{-1} band to the presence of alumina formed at that step. However, this alumina origin was discarded due to the absence of the band in the spectrum of a mixture of zeolite beta and 20% alumina activated at 673 K. An infrared band similar to the one we describe at about 890 cm^{-1} was reported in activated silicalite, and attributed to siloxane bridges formed by dehydration of two vicinal silanols.^{13,14} In our opinion, the origin of the band at 885 cm^{-1} in beta zeolite is different because of the direct relationship with the hydroxy group at 3782 cm^{-1} , which is lacking in silicalite.

The 3782 cm^{-1} band has already been assigned to a hydroxy group attached to a tricoordinated aluminum atom linked to the network via two oxygen bonds.^{24,36} Such a configuration would be obtained by the hydrolysis of Al–O bonds of a bridged aluminum in the framework upon calcination or steaming. This type of site has also been suggested to justify the presence of “invisible” aluminum atoms in NMR.²¹ Such a tricoordinated aluminum would also bear an electronic vacancy which would give it a strong Lewis acidity. Coordination of pyridine to this

SCHEME 1



aluminum atom up to high temperature would indirectly perturb the hydroxyl at 3782 cm^{-1} . Our results are in good agreement with this hypothesis: we assign the 880 cm^{-1} band to the vibration of a site with a tricoordinated aluminum (thus being a coordinatively unsaturated site) linked to the hydroxy group whose $\nu(\text{OH})$ is at 3782 cm^{-1} . A Si–O distortion similar to that in siloxane bridges in silicalite (band at 890 cm^{-1}) or in Si–O bond in Ti–silicalite (960 cm^{-1}) explains the shift of the Si–O or Si–O–Al from their normal frequencies. Adsorption of pyridine induces rearrangement of the aluminum atom in tetrahedral conformation (Scheme 1) and relaxation of the distorted group (with a shift back to their normal position for the corresponding vibrations).

CO_2 Adsorption. Formation of carbonates upon adsorption of CO_2 on beta zeolite was reported to us by Fajula.⁴⁰ To clarify the intriguing presence of basic sites on the surface of an acidic catalyst, we studied the species formed by CO_2 adsorption and the nature of the involved sites. We observed the formation of hydrogen–carbonates, which necessitates the presence of basic hydroxy groups. On alumina, hydrogen–carbonates formation was proposed on sites where a basic hydroxyl is carried by an aluminum atom next to the Al on which CO_2 is adsorbed.³³ According to Lowenstein’s rule, such a configuration cannot exist in zeolites, but the hydroxyl band at 3782 cm^{-1} which we suppose is associated to the aluminum coordination site is nevertheless perturbed when hydrogen–carbonates are formed. Association of this hydroxy group to the coordinatively unsaturated aluminum could form the acid–base pair which the hydrogen–carbonates formation necessitates: on sample BEA500, where 880 and 3782 cm^{-1} bands are observed, the amount of hydrogen–carbonates formed is more important than on the BEA900 sample, on which these bands are absent. In this case another hydrogen–carbonate source might exist, for example amorphous silica–alumina (which this highly dealuminated sample probably contains).

5. Conclusions

A new band at 880 cm^{-1} was detected in beta zeolites, together with a $\nu(\text{OH})$ vibration at 3782 cm^{-1} . Adsorption of probe molecules led to the assignment of this infrared pattern to a tricoordinated aluminum atom partly bound to the network, and to which a hydroxy group is attached. These two bands are a true infrared fingerprint of a Lewis site in zeolites, which opens new ways for the in situ study of Lewis sites in working catalysts. Evaluation of the role of this site in the coking of beta zeolites by hydrocarbon conversion is currently in progress. The second main result is the evidence given for basic sites in a fully protonated zeolite. Basic sites in the direct neighborhood

of strong Brønsted sites of protonic form zeolite could lead to a synergistic effect and contribute to the catalytic activity of the solid.

Acknowledgment. The financial support of Rhodia Chimie is gratefully acknowledged.

References and Notes

- (1) Borreto, L.; Cambor, M. A.; Corma, A.; Perez-Pariente J. *Appl. Catal.* **1992**, 82, 37.
- (2) Reddy, K. S. N.; Rao, B. S.; Shiralkar, V. P. *Appl. Catal.* **1993**, 95, 53.
- (3) Jansen J. C.; Creighton, E. J.; Njo, S. L.; van Koningsveld, H.; van Bekkum, H. *Catal. Today* **1997**, 38, 205.
- (4) Spagnol M.; Gilbert L.; Alby, D. *Ind. Chem. Lib.* **1996**, 8, 29.
- (5) Gunnewegh, E. A.; Downing, R. S.; van Bekkum, H. *Stud. Surf. Sci. Catal.* **1995**, 97, 447.
- (6) Pandey, K. A.; Singh, A. P. *Catal. Lett.* **1997**, 44, 129.
- (7) Ma, Y.; Wang, Q. L.; Jiang, W.; Zuo, B. *Appl. Catal. A* **1997**, 165, 199.
- (8) Tarakeshwar, D.-P.; Lee, J. Y.; Kim, K. S. *J. Phys. Chem.* **1998**, 102, 13.
- (9) Morrow, B. A.; Cody, I. A. *J. Phys. Chem.* **1976**, 77, 1465.
- (10) Morrow, B. A.; Cody, I. A. *J. Phys. Chem.* **1976**, 80, 1998.
- (11) Benaissa, M.; Lavalley, J. C. *J. Chem. Soc. Chem. Commun.* **1984**, 908.
- (12) Benaissa, M.; Lavalley, J. C. *Stud. Surf. Sci. Catal.* **1985**, 21, 251.
- (13) Zecchina, A.; Bordiga, S.; Spoto, G.; Marchese, L.; Petrini, G.; Leofanti, G.; Padovan, M. *J. Phys. Chem.* **1992**, 96, 4991.
- (14) Pel'menschikov, A. G.; Morosi, G.; Gamba, A.; Zecchina, A.; Bordiga, S.; Paukshtis, E. A. *J. Phys. Chem.* **1993**, 96, 11979.
- (15) Scarano, D.; Zecchina, A.; Bordiga, S.; Geobaldo, F.; Spoto, G.; Petrini, G.; Leofanti, G.; Padovan, M.; Tozzola, G. *J. Chem. Soc., Faraday Trans.* **1993**, 89(22), 4123.
- (16) Huybrechts, D. R. C.; Buskens, Ph. L.; Jacobs P. A. *J. Mol. Catal.* **1992**, 71, 129.
- (17) Cambor, M. A.; Corma, A.; Perez-Pariente, J. *J. Chem. Soc. Chem. Commun.* **1993**, 557.
- (18) Boccuti, M. R.; Rao, K. M.; Zecchina, A.; Leofanti, G.; Petrini, G. *Stud. Surf. Sci. Catal.* **1989**, 48, 133.
- (19) Bellussi, G.; Carati, A.; Clerci, G. M.; Maddellini, G.; Millini, R. *J. Catal.* **1992**, 133, 220.
- (20) Papai, I.; Goursot A.; Fajula, F.; Weber, J. *J. Phys. Chem.* **1994**, 98, 4654.
- (21) Bourgeat-Lami, E.; Massiani, P.; Di Renzo, F.; Espiau P.; Fajula, F. *Appl. Catal.* **1991**, 72, 139.
- (22) de Menorval, L. C.; Buckermann, W.; Figueras F.; Fajula, F. *J. Phys. Chem.* **1996**, 100, 465.
- (23) Beck, L. W.; Haw, J. F. *J. Phys. Chem.* **1995**, 99, 1076.
- (24) Kiricsi, I.; Flego, C.; Pazzuconi, G.; Parker, W. O.; Millini, R.; Perego C.; Bellusi, G. *J. Phys. Chem.* **1994**, 98, 4627.
- (25) Caullet, P.; Hazm, J.; Guth, J. L.; Joly, J. F.; Lynch, J.; Raatz, F. *Zeolites* **1992**, 12, 240.
- (26) Maache, M.; Janin A.; Lavalley, J. C.; Joly, J. F.; Benazzi, E. *Zeolites* **1993**, 13, 419.
- (27) Janin, A.; Maache, M.; Lavalley, J. C.; Joly, J. F.; Raatz, F.; Szydlowski, N. *Zeolites* **1991**, 11, 391.
- (28) Bocuzzi, F.; Colluccia, S.; Ghiotti, G.; Morterra, C.; Zecchina, A. *J. Phys. Chem.* **1978**, 82, 1298.
- (29) van Santen, R. A. *Stud. Surf. Sci. Catal.* **1994**, 85, 273.
- (30) Jia, C.; Massiani, P.; Barthomeuf, D. *J. Chem. Soc., Faraday Trans.* **1993**, 89(19), 3659.
- (31) Morterra, B.; Zecchina, A.; Coluccia, S. *Faraday Trans.* **1977**, 1544.
- (32) Parkyns, N. D. *J. Phys. Chem.* **1971**, 75, 526.
- (33) Parkyns, N. D. *J. Chem. Soc. A* **1969**, 410.
- (34) Coutanceau, C.; Da Silva, J. M.; Alvarez, M. F.; Ribeiro, F. R.; Guisnet, M. *J. Chim. Phys.* **1997**, 94, 765.
- (35) Loeffler, E.; Lohse, U.; Peuker, C.; Oehlmann, G.; Kustov, L. M.; Zholobenko, V. L.; Kazansky, V. B. *Zeolites* **1990**, 10, 266.
- (36) Yang C.; Xu Q. *Zeolites* **1997**, 19, 404.
- (37) Perez-Pariente, J.; Sanz, J.; Fornes, V.; Corma, A. *J. Catal.* **1990**, 124, 217.
- (38) Khabtoui, S.; Chevreau, T.; Lavalley, J. C. *Micropor. Mater.* **1994**, 3, 133.
- (39) Su B. L.; Norberg, V. *Zeolites* **1997**, 19, 65.
- (40) Fajula, F. Unpublished work.